

Structure of the Protein Phosphatase 2A Holoenzyme

Yanhui Xu,^{1,3} Yongna Xing,^{1,3} Yu Chen,^{1,3} Yang Chao,^{1,3} Zheng Lin,¹ Eugene Fan,¹ Jong W. Yu,¹ Stefan Strack,² Philip D. Jeffrey,¹ and Yigong Shi^{1,*}

¹Department of Molecular Biology, Lewis Thomas Laboratory, Princeton University, Princeton, NJ 08544, USA

²Department of Pharmacology, University of Iowa Carver College of Medicine, Iowa City, IA 52242, USA

³These authors contributed equally to this work.

*Contact: ygshi@princeton.edu

DOI 10.1016/j.cell.2006.11.033

SUMMARY

Protein Phosphatase 2A (PP2A) plays an essential role in many aspects of cellular physiology. The PP2A holoenzyme consists of a heterodimeric core enzyme, which comprises a scaffolding subunit and a catalytic subunit, and a variable regulatory subunit. Here we report the crystal structure of the heterotrimeric PP2A holoenzyme involving the regulatory subunit B'/B56/PR61. Surprisingly, the B'/PR61 subunit has a HEAT-like (huntingtin-elongation-A subunit-TOR-like) repeat structure, similar to that of the scaffolding subunit. The regulatory B'/B56/PR61 subunit simultaneously interacts with the catalytic subunit as well as the conserved ridge of the scaffolding subunit. The carboxyterminus of the catalytic subunit recognizes a surface groove at the interface between the B'/B56/PR61 subunit and the scaffolding subunit. Compared to the scaffolding subunit in the PP2A core enzyme, formation of the holoenzyme forces the scaffolding subunit to undergo pronounced conformational rearrangements. This structure reveals significant ramifications for understanding the function and regulation of PP2A.

INTRODUCTION

Controlled protein phosphorylation and dephosphorylation are a fundamental regulatory mechanism in all aspects of biology (Hunter, 1995). Protein phosphatase 2A (PP2A) is a major serine/threonine phosphatase involved in many essential aspects of cellular function (Janssens and Goris, 2001; Lechward et al., 2001; Virshup, 2000). PP2A plays an important role in cell-cycle regulation, cell-growth control, development, regulation of multiple signal transduction pathways, cytoskeleton dynamics, and cell mobility.

The PP2A core enzyme consists of a 65 kDa scaffolding protein known as A or PR65 subunit and a 36 kDa catalytic subunit or C subunit. To gain full activity towards specific

substrates, the PP2A core enzyme associates with a variable regulatory subunit to form a heterotrimeric holoenzyme. The variable regulatory subunits have four subfamilies: B (PR55), B' (B56 or PR61), B'' (PR72), and B''' (PR93/PR110), with at least 16 members in these subfamilies (Janssens and Goris, 2001; Lechward et al., 2001). In mammalian cells, the scaffolding and the catalytic subunits each have two isoforms, which share high sequence similarity (Arino et al., 1988; Green et al., 1987; Hemmings et al., 1990; Stone et al., 1987). In contrast, the sequence similarity among the four subfamilies of regulatory subunits is very low, and the expression levels of various regulatory subunits are highly diverse depending upon cell types and tissues (Janssens and Goris, 2001; Lechward et al., 2001). In this regard, the B subunits determine the substrate specificity as well as the spatial and temporal functions of PP2A.

PP2A is also an important tumor suppressor protein (Janssens et al., 2005). Mutations in the scaffolding subunit that result in compromised binding to the regulatory or catalytic subunit of PP2A, or a total absence or substantial reduction of the scaffolding subunit, had been reported to be linked to a variety of primary human tumors (Calin et al., 2000; Colella et al., 2001; Ruediger et al., 2001a; Suzuki and Takahashi, 2003; Takagi et al., 2000; Wang et al., 1998). In addition, an amino-terminally truncated form of the B subunit PR61/B'γ1 was found to be associated with a higher metastatic state of melanoma cells (Ito et al., 2000, 2003; Koma et al., 2004), while gain- and loss-of-function experiments firmly established this regulatory subunit as a tumor suppressor (Chen et al., 2004).

The PP2A scaffolding subunit contains 15 tandem repeats of a conserved 39-residue sequence known as a HEAT (huntingtin-elongation-A subunit-TOR) motif (Hemmings et al., 1990; Walter et al., 1989). These 15 HEAT repeats are organized into an extended, L-shaped molecule (Groves et al., 1999). The catalytic subunit recognizes one end of the elongated scaffolding subunit by interacting with the conserved ridges of HEAT repeats 11–15 (Ruediger et al., 1992, 1994; Xing et al., 2006). Formation of the PP2A core enzyme results in significant bending of the HEAT repeats 12–15 towards the amino terminus of the scaffolding subunit (Xing et al., 2006).

Despite recent advances, mechanistic understanding on the function and assembly of the PP2A holoenzyme has been slow to emerge. There is no structural information on any of the regulatory subunits, and it remains unclear how the regulatory subunit specifically recognizes the scaffolding subunit or the catalytic subunit. Methylation of the carboxyterminus of the catalytic subunit is thought to play an important role in the formation of a holoenzyme (Bryant et al., 1999; Kloeker et al., 1997; Tolstykh et al., 2000; Wei et al., 2001; Wu et al., 2000; Xing et al., 2006; Yu et al., 2001), although the molecular basis underlying these observations remains unclear.

In this manuscript, we report the crystal structure of a PP2A holoenzyme, involving the α isoform of the scaffolding subunit ($A\alpha$), the α isoform of the catalytic subunit ($C\alpha$), and the $\gamma 1$ isoform of the regulatory B'/B56/PR61 subunit ($B'\text{-}\gamma 1$). This crystal structure reveals a number of unexpected findings that have significant biological implications for understanding the mechanisms and cellular functions of PP2A.

RESULTS

Assembly and Crystallization of the PP2A Holoenzyme

The PP2A core enzyme, involving the full-length $A\alpha$ and $C\alpha$, was assembled as described (Xing et al., 2006). The PP2A core enzyme was methylated by a PP2A-specific leucine carboxyl methyltransferase (LCMT) in the presence of S-adenosyl methionine (SAM). The fully methylated PP2A core enzyme was incubated with a stoichiometric amount of the full-length $B'\text{-}\gamma 1$. The heterotrimeric PP2A holoenzyme was purified to homogeneity by gel-filtration chromatography.

The PP2A holoenzyme was incubated with 1.2 molar equivalence of microcystin-LR (MCLR) prior to crystallization. We succeeded in obtaining small crystals of the PP2A holoenzyme and were able to generate large, diffraction-quality crystals using macroseeding. These crystals were sensitive to radiation damage and diffracted X-rays to about 3.3 Å resolution at synchrotron. The structure was determined by a combination of molecular replacement and single-wavelength anomalous dispersion. The atomic model of the native holoenzyme has been refined to 3.3 Å resolution (Table 1).

Overall Structure of the PP2A Holoenzyme

The structure of the PP2A holoenzyme exhibits a compact architecture, measuring $90 \times 90 \times 70 \text{ \AA}^3$ (Figure 1). $A\alpha$ has an extensive, C-shaped structure characterized by double-layered α helices. Compared to the free form (Groves et al., 1999) and the PP2A core enzyme (Xing et al., 2006), $A\alpha$ has undergone significant conformational rearrangements (discussed in detail later). There are 15 HEAT repeats in $A\alpha$, with each HEAT repeat comprising a pair of antiparallel α helices. The interhelical region within each HEAT repeat forms a contiguous ridge—hereafter referred to as the ridge. As previously shown (Xing et al.,

2006), $C\alpha$ binds to one end of the scaffold through interactions with the ridge of HEAT repeats 11–15 (Figure 1), consistent with an earlier prediction (Ruediger et al., 1992). Interactions between $A\alpha$ and $C\alpha$ result in the burial of 2072 Å² exposed surface area.

The regulatory B'/PR61- $\gamma 1$ subunit has an elongated, superhelical structure comprising 18 α helices (Figure 1A). The superhelical structure has an apparent curvature, with the convex side binding to $A\alpha$ and the concave side facing up and tilted towards $C\alpha$. Strikingly, despite a complete lack of sequence homology, the structure of $B'\text{-}\gamma 1$ closely resembles that of $A\alpha$. There are eight HEAT-like repeat motifs in $B'\text{-}\gamma 1$.

$B'\text{-}\gamma 1$ makes extensive interactions with both $A\alpha$ and $C\alpha$ (Figure 1). On one hand, $B'\text{-}\gamma 1$ binds to the conserved ridge of HEAT repeats 2–8 in $A\alpha$. On the other hand, $B'\text{-}\gamma 1$ makes direct interactions with three surface areas of $C\alpha$, including helix $\alpha 5$ and the carboxyterminus. A total surface area of 4300 Å² is buried as a result of interaction between the regulatory $B'\text{-}\gamma 1$ subunit and the PP2A core enzyme. Approximately 55% of the buried surface area is due to interactions between $B'\text{-}\gamma 1$ and $C\alpha$, with the rest coming from interactions between $B'\text{-}\gamma 1$ and $A\alpha$. Interestingly, the carboxyterminus of $C\alpha$ recognizes a surface groove at the interface between $B'\text{-}\gamma 1$ and $A\alpha$ (Figure 1B).

Structure of the Regulatory B'/PR61 Subunit

The regulatory B'/PR61- $\gamma 1$ subunit consists exclusively of α helices (Figures 2 and 3). Eighteen α helices stack against each other laterally to create an elongated, superhelical structure. The concave side of the curved superhelical structure is enriched with negatively charged amino acids, whereas the convex side contains a number of conserved hydrophobic residues (Figure 2A). These hydrophobic amino acids make important contributions in binding to the scaffolding subunit $A\alpha$.

One unanticipated finding from the structural investigation is that the structure of $B'\text{-}\gamma 1$ resembles that of $A\alpha$. Systematic structure-based search of the Protein Data Bank using the DALI server (Holm and Sander, 1993) led to the identification of a number of close structural homologs, among which the nuclear import factor karyopherin α (Conti et al., 1998), the armadillo repeat protein β -catenin (Huber et al., 1997), and $A\alpha$ of PP2A (Groves et al., 1999) have the highest Z scores (similarity score) (Figure 2B). Intriguingly, both karyopherin α and β -catenin have the ability to interact with peptides using a concave surface (Conti et al., 1998; Graham et al., 2000). This analysis suggests the possibility that the regulatory B'/PR61 subunit may interact with PP2A substrates or other regulatory proteins using the acidic, concave surface (Figure 2B).

Structure of $B'\text{-}\gamma 1$ can be superimposed with that of $A\alpha$ with a root-mean-square deviation (rmsd) of 5.1 Å over 254 aligned backbone alpha carbon atoms. This alignment identified 8 HEAT-like repeats in $B'\text{-}\gamma 1$. Unlike the HEAT repeats in $A\alpha$ or the armadillo motifs in β -catenin, these

Table 1. Statistics from Crystallographic Analysis

Holoenzyme	Native	SeMet (A α & C α)	SeMet (A α & C α)
Protein components	A α , B'- γ 1, C α	A α , B'- γ 3, C α (T)	A α , B'- γ 1, C α (T)
Space group	P212121	P212121	P212121
Resolution (outer shell) (Å)	100–3.3 (3.42–3.30)	100–3.6 (3.73–3.60)	100–3.8 (3.94–3.80)
Total observations	443,360	912,830	261,894
Unique observations	70,289	53,992	45,951
Data coverage (outer shell)	99.9% (99.9%)	99.9% (100.0%)	99.7% (99.9%)
R _{sym} (outer shell)	0.104 (0.444)	0.116 (0.446)	0.109 (0.432)
Refinement			
Resolution (outer shell) (Å)	100–3.3 (3.42–3.30)	100–3.6 (3.73–3.60)	100–3.8 (3.94–3.80)
Number of reflections (F > 0)	70,199	53,472	46,983
Data coverage	98.4%	97.4%	99.6%
R _{work} (outer shell)	0.252 (0.392)	0.267 (0.364)	0.282 (0.332)
R _{free} (outer shell)	0.297 (0.434)	0.331 (0.439)	0.335 (0.418)
Total number of atoms	20,474	20,212	20,212
Number of waters	0	0	0
Rmsd bond length (Å)	0.0083	0.010	0.011
Rmsd bond angles (degree)	1.38	1.53	1.56
Average B factor			
A α —two copies per a.u.	69.6, 60.1	70.3, 48.1	81.3, 67.3
C α —two copies per a.u.	72.7, 70.1	69.2, 59.5	80.3, 76.4
B'- γ —two copies per a.u.	85.8, 79.1	84.3, 70.5	95.2, 86.3
Ramachandran Plot			
Most favored (%)	80.6	75.3	73.2
Additionally allowed (%)	17.6	22.5	23.8
Generously allowed (%)	1.4	2.0	2.5
Disallowed (%)	0.3	0.3	0.4

$R_{sym} = \frac{\sum_h \sum_i |I_{h,i} - I_h|}{\sum_h \sum_i I_{h,i}}$, where I_h is the mean intensity of the i observations of symmetry-related reflections of h . $R = \frac{\sum |F_o - F_c|}{\sum F_o}$ where $F_o = F_p$, and F_c is the calculated protein structure factor from the atomic model (R_{free} was calculated with 5% of the reflections). Rmsd in bond lengths and angles are the deviations from ideal values. In protein components, C α (T) represents the trypsin-digested C α (residues 1–294), which has the C-terminal 15 amino acids removed.

HEAT-like motifs exhibit little sequence homology and appear to lack a strong consensus sequence (Figure 3). Nonetheless, these motifs can be superimposed with each other with 0.9–2.5 Å pairwise rmsd (Figures 2C and 3). HEAT-like motif 7 of B'- γ 1 is most homologous to the HEAT repeat of A α . For the ease of discussion, the HEAT-like motifs of B'- γ 1 are hereafter referred to as HEAT repeats.

Interface between the Catalytic and the Regulatory Subunits

The interface between the catalytic subunit and the regulatory B'/PR61 subunit is extensive and consists of two major areas (Figure 4A). In one area, amino acids from HEAT repeats 6–8 of B'- γ 1 interact with residues in the

α 5 region of C α , mainly through hydrogen bonds (Figure 4B). At the center of this interface, the polar side chain of Gln125 in C α makes a pair of hydrogen bonds to the main chain atoms in B'- γ 1. The aliphatic portion of Gln125 side chain also mediates van der Waals contact with His339, Phe340, and Trp382 in B'- γ 1. These interactions are further buttressed by three hydrogen bonds between the side chain of Asp131 in C α and the amide nitrogen and side chain of Ser298 in B'- γ 1 (Figure 4B).

In the other area, the hydrophobic carboxyl terminus of C α is nestled in a surface groove at the interface between A α and B'- γ 1 (Figure 4C). There are numerous van der Waals contacts at this interface. Three residues from C α , Pro305, Tyr307, and Phe308, stack closely against each other and are surrounded by the aliphatic portion of the

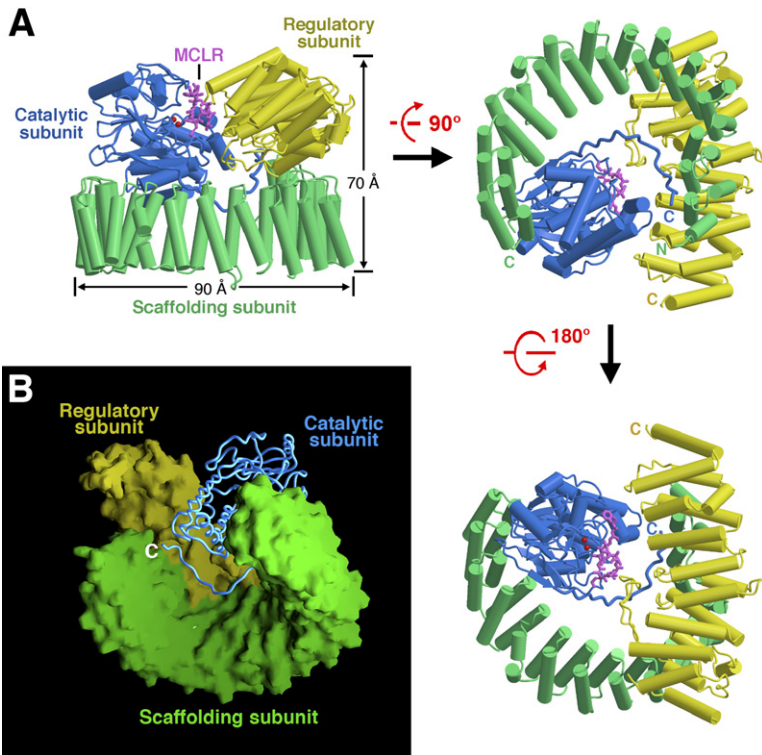


Figure 1. Overall Structure of the Heterotrimeric PP2A Holoenzyme Bound to Microcystin-LR (MCLR)

(A) Overall structure of the PP2A holoenzyme bound to MCLR. The scaffolding ($A\alpha$), catalytic ($C\alpha$), and regulatory $B'/PR61$ ($B'-\gamma 1$) subunits are shown in green, blue, and yellow, respectively. MCLR is shown in magenta. $B'-\gamma 1$ interacts with both $A\alpha$ and $C\alpha$ through extensive interfaces. $C\alpha$ interacts with $A\alpha$ as described (Xing et al., 2006). Three views are shown here to reveal the essential features of the holoenzyme. Surprisingly, $B'-\gamma 1$ adopts a structure that closely resembles that of the scaffolding subunit (discussed in detail later).

(B) A surface representation of the PP2A holoenzyme. $A\alpha$ and $B'-\gamma 1$ are shown in surface representation. $C\alpha$ is shown in backbone worm to highlight the observation that the carboxyl terminus of $C\alpha$ binds to a surface groove at the interface between $A\alpha$ and $B'-\gamma 1$. Figures 1A, 2A, 4A, and 4E were prepared using GRASP (Nicholls et al., 1991); all other structural figures were made using MOLSCRIPT (Kraulis, 1991).

side chains of Lys256, Lys 258, Tyr292, and Lys295 in $B'-\gamma 1$ and Asp63, Glu64, and Glu101 of $A\alpha$ (Figure 4C). These van der Waals interactions are strengthened by six additional hydrogen bonds, one of which occurs between the side chain of Glu64 in $A\alpha$ and the main chain amide nitrogen of residue 309 in $C\alpha$ (Figure 4C). Importantly, mutation of Glu64 to Asp or Gly in $A\alpha$ has been observed

in cancer cells (Ruediger et al., 2001b). Supporting an important role for Glu64, the mutant proteins E64D and E64G exhibited significantly compromised ability to interact with the $B'/PR61$ subunit (Ruediger et al., 2001b). Our structural observation provides a rational basis for the mutagenesis result and for the cancer link. Although the carboxylate of Leu309 is fully methylated as judged by

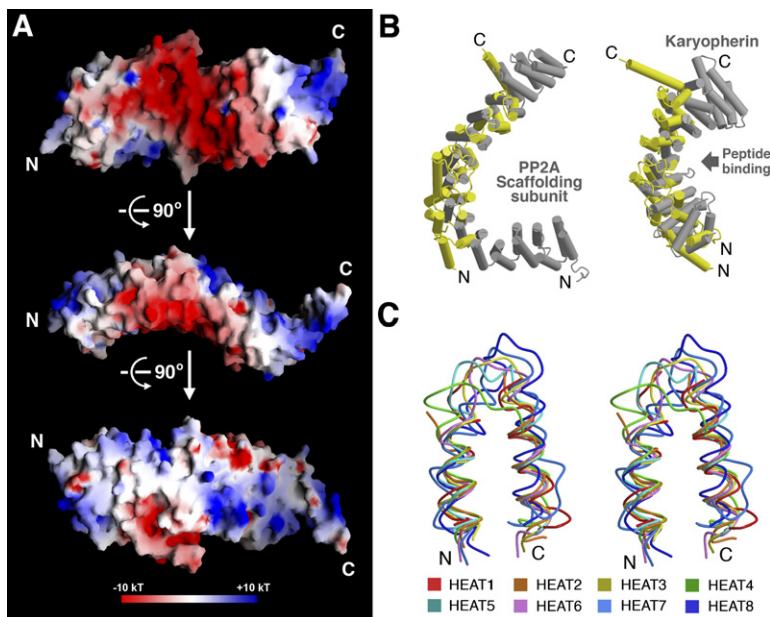


Figure 2. Structure of the Regulatory $B'/PR61$ Subunit

(A) A surface representation of the structure of $B'-\gamma 1$ showing electrostatic potential. Three perpendicular views are shown here. Note that the elongated $B'-\gamma 1$ protein contains a highly acidic, concave surface patch (top panel). $B'-\gamma 1$ uses its less-charged, convex surface to interact with $A\alpha$.

(B) The regulatory $B'/PR61$ subunit is structurally similar to the scaffolding subunit of PP2A and other binding proteins. $B'-\gamma 1$ (yellow) contains eight HEAT repeat-like structural motifs. These HEAT-like motifs can be superimposed well with the scaffolding subunit of PP2A (left panel) or karyopherin α (importin α , right panel). The peptide binding region of karyopherin α coincides with the acidic, concave surface of $B'-\gamma 1$.

(C) Structural overlay of all eight HEAT-like motifs in the regulatory $B'/PR61$ subunit. HEAT-like motif 7 is most similar to the HEAT repeat of the PP2A scaffolding subunit. The majority of the HEAT-like motifs have helices almost parallel with each other.

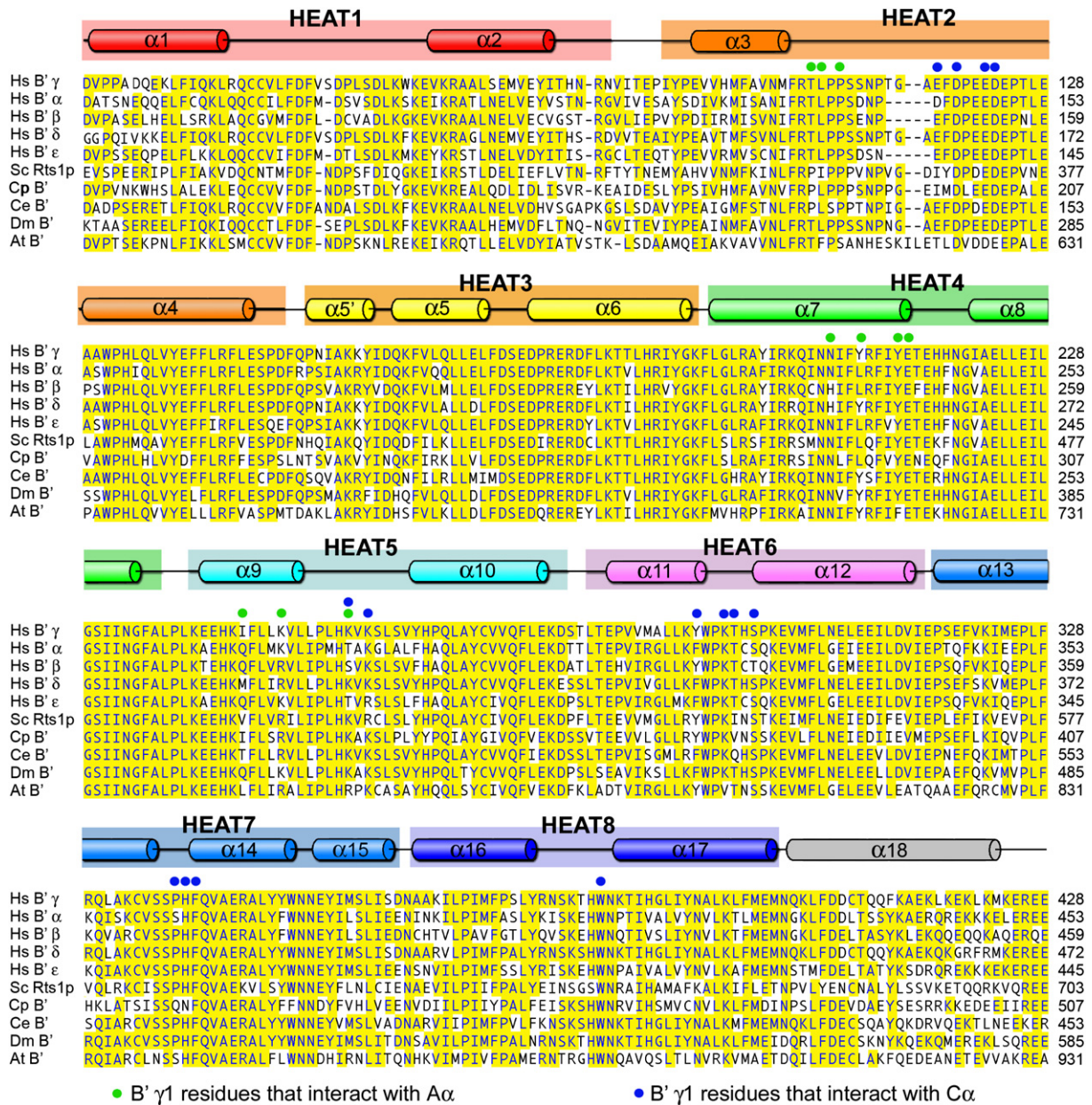


Figure 3. Sequence Alignment of the Regulatory B'/PR61 Subunits across Species

Secondary structural elements are indicated above the sequences. Each HEAT repeat is represented by a distinct color. Conserved residues are highlighted in yellow. Residues that interact with A α and C α are identified by green and blue circles, respectively, above the sequences. The sequences shown include all five isoforms of B'/PR61 from humans: alpha (GI:18490281), beta (GI:30795206), gamma1 (GI:1418819), delta (GI:31083279), and epsilon (GI:31083295). The other sequences are the following: *Saccharomyces cerevisiae* Rts1p (GI:532526), *Chizosaccharomyces pombe* CpB' (GI:19075706), *Caenorhabditis elegans* CeB' (GI:17557914), *Drosophila melanogaster* DmB' (GI:60677747), and *Arabidopsis thaliana* AtB' (GI:2244898). Residues 626–651 were not shown in this alignment.

Western blot, we chose not to build the methyl group, because the electron density for the methyl group is weak. Nonetheless, the binding groove for the carboxyl terminus of C α is very acidic (Figure 4A); methylation of the carboxyl terminus of C α removes a negative charge and presumably facilitates its docking into the acidic groove.

In addition to the two major interfaces, the extended loop within HEAT repeat 2 of B'- γ 1 makes additional interactions with C α . Arg268 of C α , which mediates van der Waals contacts with MCLR, donates three hydrogen bonds to residues in B'- γ 1: two to the main chain carbonyl oxygen atoms of residues 119 and 122 and one to the side chain of Asp123 (Figure 4D).

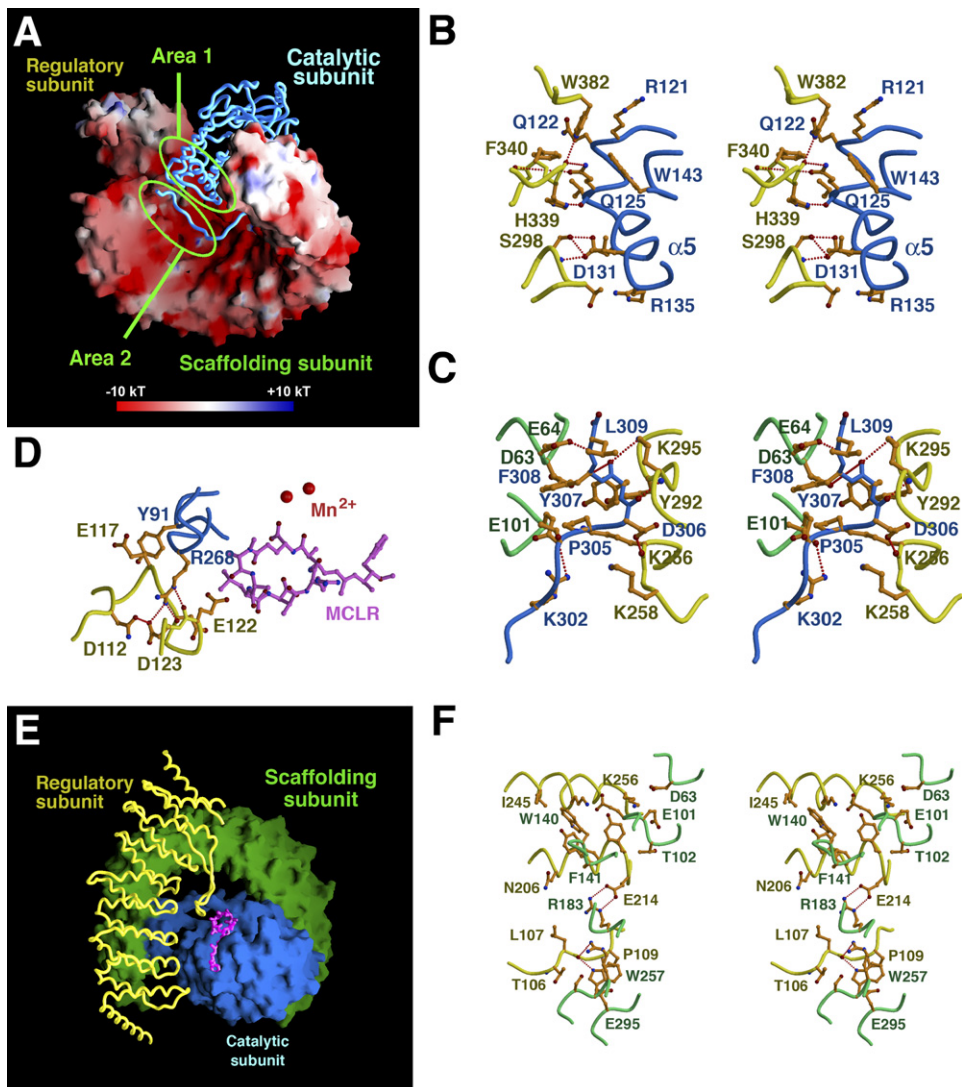


Figure 4. Interactions among the Three Components of the PP2A Holoenzyme

(A) A surface potential representation of the PP2A holoenzyme. The electrostatic surface potential is shown for $A\alpha$ and $B'\text{-}\gamma 1$. Note the acidic environment at the interface between $A\alpha$ and $B'\text{-}\gamma 1$. The carboxyl terminus of $C\alpha$ extends out into a negatively charged surface groove at the interface between $A\alpha$ and $B'\text{-}\gamma 1$. Two areas are circled. Area 1 involves a protein interface between $C\alpha$ and $B'\text{-}\gamma 1$. Area 2 centers on the recognition of the carboxyl terminus of $C\alpha$ by $A\alpha$ and $B'\text{-}\gamma 1$.

(B) A stereo view of the atomic interactions between $C\alpha$ and $B'\text{-}\gamma 1$ in area 1. This interface involves the HEAT-like repeats 6–8 of $B'\text{-}\gamma 1$ and the $\alpha 5$ helix region of $C\alpha$. Side chains are colored orange. This interface contains a number of hydrogen bonds, which are represented by red dashed lines.

(C) A stereo view of the recognition of the carboxyl terminus of $C\alpha$ by $A\alpha$ and $B'\text{-}\gamma 1$ in area 2. This interface involves the HEAT-like repeats 5 and 6 of $B'\text{-}\gamma 1$ and HEAT repeats 1 and 2 of $A\alpha$. Most residues from the carboxyl terminus of $C\alpha$ participate in specific interactions. There is a good mixture of hydrogen bonds and van der Waals interactions at this interface.

(D) Additional interactions with $C\alpha$ are provided by the extended loop within HEAT-like motif 2 of $B'\text{-}\gamma 1$.

(E) A surface representation of the PP2A holoenzyme to highlight the binding mode of the regulatory $B'/\text{PR61}$ subunit. Note that $B'\text{-}\gamma 1$ uses its convex surface to interact with the conserved ridge of $A\alpha$.

(F) A stereo view of the atomic interactions between $A\alpha$ and $B'\text{-}\gamma 1$. This interface is rich in van der Waals interactions and involves six HEAT repeats of $A\alpha$.

Interface between the Regulatory and the Scaffolding Subunits

$B'\text{-}\gamma 1$ uses its convex surface to sit on the ridge of HEAT repeats 2–8 in $A\alpha$ (Figure 4E). Although the buried surface area is large, the intensity of interaction does not appear

to be high. The interface between $B'\text{-}\gamma 1$ and $A\alpha$ is scattered into a large area and a small area. The large area involves HEAT repeats 4 and 5 of $B'\text{-}\gamma 1$ and the ridge of HEAT repeats 2–5 of $A\alpha$ (Figure 4F). Trp140 and Phe141 of $A\alpha$ make multiple van der Waals interactions with

hydrophobic residues in B'- γ 1. In addition, Arg183 of A α donates a pair of charge-stabilized hydrogen bonds to Glu214 of B'- γ 1 (Figure 4F). Lys256 of B'- γ 1 forms a salt bridge with three acidic residues in A α , Asp63, Glu100, and Glu101 (Figure 4F). The small area involves the extended loop in HEAT repeat 2 of B'- γ 1 and the ridge of HEAT repeats 7 and 8, where Trp257 of A α hydrogen bonds to main chain carbonyl oxygen of residue 107 in B'- γ 1 (Figure 4F).

All residues in B'- γ 1 that mediate important contacts with residues in C α and A α are highly conserved. For example, Glu214, which accepts two hydrogen bonds from Arg183 of A α (Figure 4F), and Asp123, which hydrogen bonds to Arg268 of C α (Figure 4D), are invariant in all B'/PR61 family members across species (Figure 3). The other three B'- γ 1 residues that contribute to hydrogen bonds at the interfaces, Lys295, Ser298, and His339, are conserved in all but one B'/PR61 family members (Figure 3). This analysis indicates that the binding interactions reported in this study are likely conserved in holoenzymes involving other B'/PR61 isoforms.

Biochemical Analysis of Subunit Interaction

PP2A is a tumor suppressor protein. Mutations in both the α and β isoforms of the scaffolding subunit have been found in cancer. Glu64 of A α was mutated to Asp in lung cancer and to Gly in breast cancer (Ruediger et al., 2001b). Several cancer-derived missense mutations have been identified in A β , including P65S, L101P, K343E, D504G, and V545A (Wang et al., 1998). These five mutations correspond to P53S, L89P, K331E, D492G, and V533A, respectively, in A α . To examine the effect of these mutations on PP2A subunit interaction, we generated mutant A α proteins, each containing one such mutation. Using a published protocol (Li and Virshup, 2002) and homogeneous recombinant proteins, we examined the effect of each mutation on interaction with the B'/PR61 regulatory subunit. Consistent with the observed important function of Glu64 in binding to B'- γ 1 (Figure 4C), mutation of Glu64 to Gly or Asp significantly compromised its binding to B'- γ 1 (Figure S1A). In contrast, mutation of Pro53, Leu89, and Lys331 of A α , which are not involved in direct interaction with B'- γ 1, did not affect binding to B'- γ 1 (Figure S1A).

We also examined the effect of mutations on the interaction between A α and C α . The conserved ridge of HEAT repeats 11–15 in A α is responsible for binding to C α . Consequently, mutation of residues (Pro53, Glu64, Leu 89, and Lys331) outside of the ridge of HEAT repeats 11–15 had no impact on the interaction between A α and C α (Figure S1B). Interestingly, however, the mutations Y456A, Y495A, and V533A, which affect residues at the interface with C α , did not significantly weaken the interaction with C α (Figure S1B). This is likely due to the fact that the interactions between A α and C α are extremely strong with a dissociation constant of about 0.1 nM (Kamibayashi et al., 1992); such interactions might be able to withstand the mild Ala mutations. Supporting this notion, the

mutation of Val533 to a charged residue Asp resulted in abrogation of the interaction between A α and C α (Figure S1B). It is noteworthy that Val533 in A α corresponds to Val545 in A β , which was mutated in colon cancer (Wang et al., 1998). Finally, mutation of Asn535, which mediates two hydrogen bonds at the interface, to Lys also abolished the interaction between A α and C α (Figure S1B).

Conformational Changes in the Scaffolding Subunit

The conformation of the free A α is well defined, with only minor variation in the carboxy-terminal HEAT repeats (Groves et al., 1999). Formation of the PP2A core enzyme resulted in a pronounced conformational change in A α , which pivots around HEAT repeat 13 (Xing et al., 2006). The core enzyme associates with a variable regulatory subunit to form a holoenzyme. To assess additional conformational changes brought about by binding to the regulatory subunit, we attempted to superimpose the core structure of the PP2A core enzyme—the entire C α and HEAT repeats 11–15—with the same fragment from the PP2A holoenzyme. This analysis revealed a drastic conformational rearrangement (Figure 5A). Formation of the holoenzyme forces the N-terminal HEAT repeats of A α to twist and to move by as much as 50–60 Å. As a result of this dramatic change, the amino and carboxyl termini of A α are now 53 Å apart from each other, compared to 70 Å in the PP2A core enzyme.

To locate the site of the conformational rearrangement, we compared the result of two alignments of A α between the core enzyme and the holoenzyme. One alignment was based on the carboxy-terminal 5 HEAT repeats (Figure 5B, left panel) whereas the other alignment relied on the amino-terminal 10 HEAT repeats (Figure 5B, right panel). This comparison revealed that, in both cases, drastic conformational rearrangement originates in the amino-terminal helix of HEAT repeat 11 (Figures 5B and 5C). Hydrophobic packing within protein interior remains unchanged for HEAT repeats 1–10 and 12–15. However, packing interactions both within HEAT repeat 11 and between HEAT repeats 11 and 10 or 12 have changed.

To accurately identify the pivoting residues, we examined this helix in atomic detail and found one significant difference. The distance between the carbonyl oxygen atom of residue 401 and the amide nitrogen atom of residue 405 is 2.9 Å in the core enzyme, suggesting a normal hydrogen bond (Figure 4D). In contrast, this distance is enlarged to 4.7 Å in the holoenzyme, which is beyond the range of a hydrogen bond (Figure 4D). Thus, the breakage of the main chain hydrogen bond between residues 401 and 405 in HEAT repeat 11 appears to make a dominant contribution to the observed conformational rearrangement. Interestingly, Pro406 is located immediately carboxy-terminal to the broken hydrogen bond; this residue likely endows the helix in HEAT repeat 11 the ability to bend.

Role of Methylation in Holoenzyme Assembly

Methylation of the carboxyl terminus of the catalytic subunit is thought to play an important role in the formation

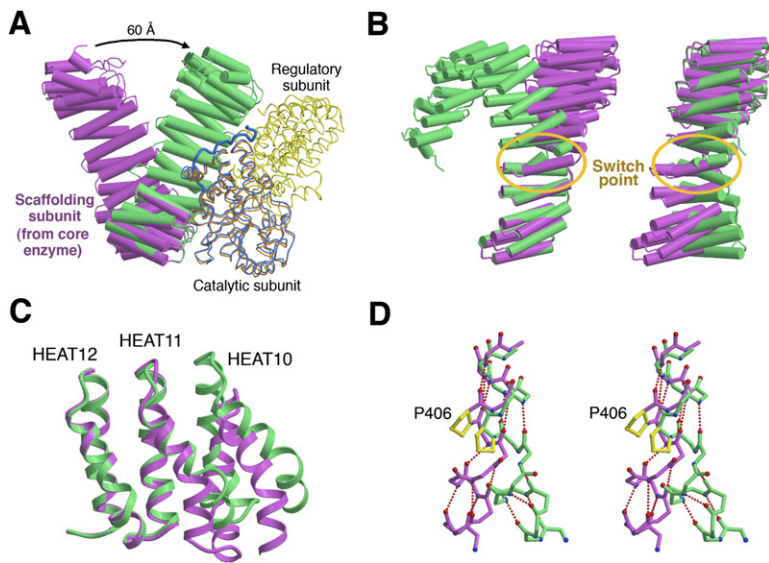


Figure 5. Remarkable Conformational Flexibility of the Scaffolding Subunit

(A) Structural comparison of the PP2A core enzyme (Xing et al., 2006) with the PP2A holoenzyme. The PP2A core enzyme contains $C\alpha$ (orange worm) and $A\alpha$ (magenta). The core enzyme is aligned with the PP2A holoenzyme to show the extent of conformational rearrangements upon binding to $B'\text{-}\gamma 1$. Compared to that in the core enzyme, the amino-terminal portion of $A\alpha$ swings as much as 50–60 Å in formation of the holoenzyme.

(B) The switch point of the conformational changes in the scaffolding subunit is in HEAT repeat 11. To locate the switch point, the scaffolding subunits from the core enzyme and the holoenzyme were aligned on the basis of their carboxy-terminal 5 HEAT repeats (left panel) and their amino-terminal 10 HEAT repeats. Comparison of these two alignments identified a single switch point in HEAT repeat 11.

(C) A close-up view of the alignment around HEAT repeat 11.

(D) A stereo view of the detailed hydrogen bond patterns in the first α helix of HEAT repeat 11. The switch in HEAT repeat 11 appears to originate from residues 401–406. The presence of Pro406 makes it an ideal candidate for allowing these conformational rearrangements to occur.

of a holoenzyme involving the regulatory subunits B/PR55 (Bryant et al., 1999; Tolstykh et al., 2000; Wei et al., 2001; Wu et al., 2000; Yu et al., 2001) and B'' /PR72 (Xing et al., 2006). For the B' /PR61 family, however, the role of methylation in holoenzyme assembly is less well characterized (Tolstykh et al., 2000; Wei et al., 2001). In fact, the B' /PR61 subunits were found to associate with the scaffolding subunit alone (Li and Virshup, 2002) or with the unmethylated PP2A core enzyme (Tolstykh et al., 2000). These observations strongly argue that methylation of the catalytic subunit facilitates but may not be required for the formation of a heterotrimeric PP2A complex involving the B' /PR61 subunits. This notion is consistent with the structural observation that the carboxy-terminal residue Leu309 does not mediate significant interactions in the PP2A holoenzyme (Figure 4C).

To investigate the role of methylation in the assembly of a PP2A holoenzyme involving the B' /PR61 subunits, we prepared three variants of the catalytic subunit: the fully methylated $C\alpha$, the unmethylated $C\alpha$, and the truncated $C\alpha$ (residues 1–294) that is missing the carboxy-terminal 15 amino acids. These $C\alpha$ variants were individually used to associate with $A\alpha$ to form the core enzymes, which were then incubated with $B'\text{-}\gamma 1$ for holoenzyme assembly as assessed by gel filtration. As anticipated, the fully methylated PP2A core enzyme formed a stable heterotrimeric complex with $B'\text{-}\gamma 1$ (Figure 6A, top panel). Interestingly, the unmethylated PP2A core enzyme and that involving the truncated $C\alpha$ also formed stable complexes with $B'\text{-}\gamma 1$ (Figure 6A, middle and bottom panels). These results unambiguously show that formation of the heterotrimeric

PP2A complex in vitro does not require methylation of $C\alpha$. Using isothermal titration calorimetry (ITC), the binding affinity between $B'\text{-}\gamma 1$, and the unmethylated PP2A core enzyme was determined to be approximately 52.6 ± 7.9 nM (Figure 6B).

Next, we crystallized the heterotrimeric PP2A complexes involving $A\alpha$, truncated $C\alpha$ (residues 1–294), and $B'\text{-}\gamma 1$ or $B'\text{-}\gamma 3$. We determined both crystal structures and refined the atomic models to 3.8 and 3.6 Å resolution, respectively (Table 1 and Figures 6C and S2). These two structures are nearly identical to each other, with an rmsd of 0.6 Å for all backbone alpha carbon atoms. Thus, we focus our discussion on one such complex. Notably, compared to the methylated PP2A holoenzyme, the absence of methylation does not appear to cause any significant structural rearrangement in the holoenzyme involving the truncated $C\alpha$, as judged by the relatively small rmsd of 0.66 Å over 1256 aligned alpha carbon atoms. The primary protein-protein interfaces between $A\alpha$ and $C\alpha$ and between $A\alpha$ and B' are also exactly preserved in the heterotrimeric PP2A complexes involving the truncated $C\alpha$. The only apparent difference is that interactions mediated by the carboxy-terminal 15 amino acids of $C\alpha$ are now absent (Figure 6C).

DISCUSSION

The heterotrimeric PP2A holoenzyme is believed to determine the substrate specificity as well as the spatial and temporal functions of PP2A. For example, the PP2A holoenzyme involving the B' /PR61 family plays an essential role

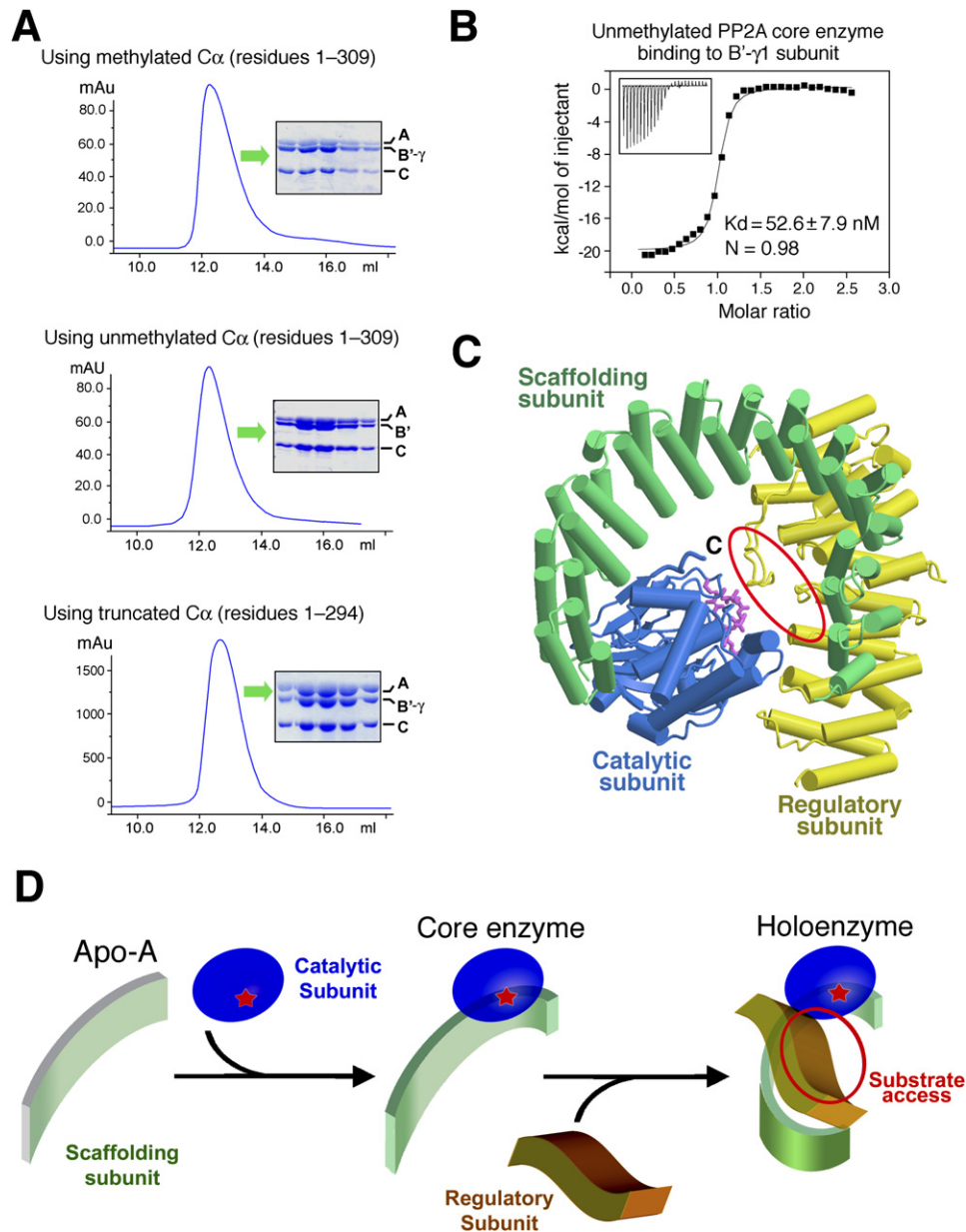


Figure 6. Role of Methylation in the Assembly of PP2A Holoenzyme Involving B'/PR61 Subunit

(A) In vitro assembly of a heterotrimeric PP2A complex does not depend on methylation of the catalytic subunit. Compared to the fully methylated $C\alpha$ (top panel), the unmethylated $C\alpha$ (middle panel) and the carboxy-terminally truncated $C\alpha$ (residues 1–294) (bottom panel) retained the ability to form a stable complex with $A\alpha$ and $B'\text{-}\gamma 1$. Shown here are representative gel-filtration runs, with the peak fractions visualized by SDS-PAGE and Coomassie blue staining.

(B) Measurement of the binding affinity between $B'\text{-}\gamma 1$ and the unmodified PP2A core enzyme using isothermal titration calorimetry (ITC).

(C) Structure of the heterotrimeric PP2A complex involving $A\alpha$ (green), $B'\text{-}\gamma 3$ (yellow), and the truncated $C\alpha$ (blue, residues 1–294). The red oval circle denotes the absence of interactions involving the carboxyl terminus of $C\alpha$.

(D) A structure-based model for the assembly and regulation of the PP2A holoenzyme. The first step in holoenzyme assembly is the association of the free scaffolding subunit with the catalytic subunit to form the PP2A core enzyme. This association results in significant conformational changes in HEAT repeats 13 and to a lesser extent HEAT repeat 12 (Xing et al., 2006). The PP2A core enzyme then associates with a regulatory B'/PR61 subunit to form a holoenzyme. This association results in more drastic conformational rearrangements in the scaffolding subunit. The regulatory B'/PR61 subunit recruits substrate proteins using its acidic, concave groove. The red star in the catalytic subunit denotes the active site.

in cell-cycle progression, through direct interaction with the protein Shugoshin (Kitajima et al., 2006; Riedel et al., 2006; Tang et al., 2006). In this manuscript, we report the crystal structures of the PP2A holoenzyme involving the regulatory B'/PR61 subunits.

These structures reveal a number of unexpected findings. First, the structure of B'/PR61 closely resembles that of a number of other superhelical proteins, including karyopherin, β -catenin, and the scaffolding subunit of PP2A. This unexpected structural mimicry raises a number of interesting scenarios. The scaffolding subunit uses its ridge to interact with the catalytic and the regulatory subunit. Similarly, the B'/PR61 subunit uses its own ridge to bind to the catalytic subunit; in the meantime, the convex side of the B'/PR61 subunit recognizes the ridge of the scaffolding subunit. This arrangement leaves the highly acidic, concave side of B'/PR61 unoccupied. It is possible that the B'/PR61 subunit relies on the acidic, concave surface to interact with substrate proteins or peptide motifs. Consistent with this hypothesis, the concave surface is tilted towards the active site pocket of the PP2A catalytic subunit. Additional support comes from the observation that both karyopherin and β -catenin contain a charged, concave surface groove that interacts with peptides (Conti et al., 1998; Graham et al., 2000), although importin- β can also bind to peptides using its convex surface (Bayliss et al., 2000). We propose that, following the assembly of a PP2A holoenzyme involving a B'/PR61 subunit, the concave, acidic surface is used to recruit substrate proteins, which may contain a positively charged epitope (Figure 6D). Supporting this hypothesis, Shugoshin, which interacts with the B'/PR61 subunit in cell-cycle regulation, is a basic protein.

Although conformational flexibility was evident from the study of the PP2A core enzyme (Xing et al., 2006), the pronounced structural changes upon formation of the holoenzyme is still unanticipated. When the core domains of the PP2A core enzyme are aligned, the amino-terminal HEAT repeats of the scaffolding subunit swing by as much as 50–60 Å. Through structural analysis, we located the switch point to be within the first helix of HEAT repeat 11 and mapped the helix-breaking amino acids to be within residues 401–406. The characteristic presence of proline in the HEAT repeats is believed to cause the bending of helices in the outer layer and subsequent formation of the horse-shoe shaped scaffolding subunit (Groves et al., 1999). Here, the presence of proline in HEAT repeat 11 is likely to be a major source of the observed conformational flexibility, which is likely essential for PP2A function. The PP2A core enzyme must specifically associate with four different classes of the regulatory subunits and must act to remove phosphate groups in different substrates; having conformational latitude may facilitate binding to regulatory subunits and help accomplish catalysis.

Our structural analysis provides a mechanistic basis for a body of published data on the assembly of PP2A holoenzyme (Kamibayashi et al., 1992, 1994; Li and Virshup, 2002; Ruediger et al., 1992, 1994). HEAT repeats 1–10

were found to be required for interaction with the regulatory subunit (Ruediger et al., 1994). Our structural analysis shows, however, only HEAT repeats 2–8 of $A\alpha$ are directly involved in binding to B'/PR61. One plausible explanation for the difference is that HEAT repeats 1, 9, and 10 might be important for the structural integrity of HEAT repeats 2–8. Supporting this explanation, a mutant $A\alpha$ with truncation of the first HEAT repeat exhibited poor solution behavior and failed to assemble into a holoenzyme (data not shown).

Two regions of the regulatory B'/B56/PR61 subunits were found to mediate binding to the scaffolding subunit of PP2A (Li and Virshup, 2002). One of these regions includes residues 200–303, which correspond to HEAT-like repeats 4 and 5 (Figure 3). This region contains seven amino acids that directly interact with $A\alpha$. One of the seven residues, Glu214, makes a pair of hydrogen bonds to Arg183 in $A\alpha$. Interestingly, the two regions of the B'/PR61/B56 subunits appeared to be conserved in the regulatory B/B55/PR55 and B'/PR72 subunits, with an invariant Glu corresponding to Glu214 in B'/B56/PR61 (Li and Virshup, 2002). This observation raises the possibility that some of the interactions between the scaffolding and the regulatory B'/B56/PR61 subunits may be conserved for the other two major families of regulatory subunits (Li and Virshup, 2002). However, this possibility does not necessarily imply that the other two families of regulatory subunits have similar helical structures as the B'/B56/PR61 family. In fact, B/B55/PR55 is predicted to contain multiple WD40 repeats, whereas B'/PR72 is thought to contain two calcium binding EF hands (Janssens et al., 2003).

While this paper was under review, a manuscript describing the structure of the PP2A holoenzyme was published online (Cho and Xu, 2006). This holoenzyme contains the full-length $A\alpha$, $C\alpha$, and an amino-terminally truncated B'- γ 1 (Cho and Xu, 2006). Both structures show unambiguously that the carboxy-terminal residues of $C\alpha$ contribute to the formation of PP2A holoenzyme (Figure 4C). Intriguingly, however, these interactions do not appear to be required for the assembly of a heterotrimeric PP2A complex in vitro (Figure 6). In fact, the B'/PR61 subunit can bind to $A\alpha$ in the absence of $C\alpha$ (Li and Virshup, 2002) (Figure S1A). Although these in vitro experiments may not necessarily recapitulate the circumstances in cells, the structures of the PP2A holoenzyme provide powerful references for understanding the function and regulation of PP2A.

EXPERIMENTAL PROCEDURES

Protein Preparation and Assembly of PP2A Holoenzyme

All constructs and point mutations were generated using a standard PCR-based cloning strategy. B'- γ 1 and B'- γ 3 were overexpressed in *E. coli* as a fusion protein with glutathione S transferase (GST) and purified as described (Xing et al., 2006). The PP2A core enzyme, involving the full-length $C\alpha$ (residues 1–309) and $A\alpha$ (residues 8–589), was assembled as described (Xing et al., 2006). The PP2A core enzyme was methylated by a PP2A-specific leucine carboxyl methyltransferase

(LCMT) in the presence of S-adenosyl methionine (SAM) (see below). Following complete methylation, the fully methylated PP2A core enzyme was incubated with a stoichiometric amount of B'- γ 1. The PP2A holoenzyme was purified to homogeneity by gel-filtration chromatography. In addition, the purified full-length C α was used to generate a carboxy-terminally truncated variant (residues 1–294) through trypsin digestion. The truncated C α was in turn used to form a core enzyme with A α (residues 8–589), which was then assembled into two additional PP2A holoenzyme complexes, one involving B'- γ 1 and the other involving B'- γ 3. To facilitate structure determination, we also prepared the three PP2A holoenzyme complexes using selenomethionine-substituted A α and B'- γ 1 proteins.

Crystallization and Data Collection

Diffraction crystals were obtained for the three PP2A holoenzyme complexes described above, which were individually incubated with 1.2 molar equivalence of MCLR prior to crystallization. We also generated crystals of the holoenzyme using selenomethionine-substituted scaffolding and regulatory subunits. Crystals were grown by the hanging-drop vapor-diffusion method by mixing the protein (~8 mg/ml) with an equal volume of reservoir solution containing 10%–15% PEG8000, 0.1 M Tris-Cl, pH 8.5, and 0.2 M magnesium sulfate. Small crystals appeared within a few hours. Macroseeding was used to generate single, large crystals. The crystals belong to the space group P212121, with $a = 109.29 \text{ \AA}$, $b = 159.05 \text{ \AA}$, and $c = 269.17 \text{ \AA}$. There are two complexes per asymmetric unit, and the solvent content is approximately 80%. Crystals were slowly equilibrated in a cryoprotectant buffer containing reservoir buffer plus 20% glycerol (v/v) and were flash frozen in a cold nitrogen stream at -170°C . The native and selenium SAD data sets were collected at NSLS beamline X29 and processed using the software Denzo and Scalepack (Otwinowski and Minor, 1997).

Structure Determination

The structure of human PP2A holoenzyme was determined by molecular replacement using three models: C α and two fragments of A α (residues 9–415 and 416–589) from the structure of the previously determined PP2A core enzyme (accession code 2IE3) (Xing et al., 2006). Fragments were located using the program PHASER (McCoy et al., 2005). The backbone of B'- γ was built into model-phased two-fold-averaged $2F_o - F_c$ and $F_o - F_c$ electron density maps. Side-chain interpretation was guided by model-phased anomalous difference Fouriers of SeMet SAD data collected from complexes containing SeMet-labeled A α and B' components. Model building was performed using O (Jones et al., 1991) and refined using CNS (Brunger et al., 1998). Tight NCS restraints between the two complexes (50 kcal/mol) were applied throughout most of the refinement and relaxed in the final cycles. Positional refinement was performed against maximum likelihood target with NCS- and geometrically restrained individual B factor refinement, with weights adjusted on the basis of R_{free} . In tests, this refinement method consistently gave a lower R_{free} than grouped B factor refinement (which cannot be restrained by geometry in CNS) and was considerably better than adopting a single overall or per-domain B factor model. The final atomic model of the native holoenzyme has been refined to 3.3 \AA resolution. Due to nearly identical unit cells, structures of the two heterotrimeric PP2A complexes involving the truncated C α were directly refined at 3.6 and 3.8 \AA resolution after removal of the carboxy-terminal 15 amino acids from C α . Similar positional and B factor refinement protocols were used as described above. For the native holoenzyme, the atomic model contains amino acids 2–309 for C α , residues 8–589 for A α , and residues 38–66 and 68–425 for B'- γ 1. There is no electron density for residues 1–37 and 426–439 of B'- γ 1; we presume these regions are disordered in the crystals. The methyl group on the methylated carboxyl terminus of C α was not modeled, because there is no clear electron density for this group at this resolution. For the holoenzyme involving the truncated C α (residues 1–294) and B'- γ 3 or B'- γ 1, the atomic models contain amino acids 2–294 for C α , residues 8–589 for A α , and residues 38–66 and 68–425 for B'- γ 3 or B'- γ 1.

Methylation of PP2A Core Enzyme by LCMT

LCMT and PP2A core enzyme, at a 1:2 molar ratio, was incubated on ice. Methylation was initiated by addition of SAM (S-adenosyl methionine) to a final concentration of 0.75 mM. The reaction was carried out at 22°C and reached completion after 2–3 hours. The methylated PP2A core enzyme was purified away from LCMT by anion exchange chromatography. The extent of methylation was examined using an antibody that only recognizes the unmethylated carboxyl terminus of C α (Xing et al., 2006).

GST-Mediated Pull-Down Assay

Approximately 30 μg of GST-A α were bound to 30 μl of glutathione resin. The resin was washed with 200 μl assay buffer for three times to remove excess unbound A α . Then 20 μg of wild-type (WT) or mutant B'- γ 1 were allowed to bind the resin in a 125 μl volume. After four times of washing with an assay buffer containing 25 mM Tris, pH 8.0, 150 mM NaCl, and 2 mM dithiothreitol (DTT), the remaining protein and resin were mixed with 15 μl SDS sample buffer and applied to SDS-PAGE. The results were visualized by SDS-polyacrylamide gel electrophoresis (SDS-PAGE) with Coomassie blue staining.

Isothermal Titration Calorimetry (ITC)

To obtain a direct binding affinity between PP2A core enzyme and B'- γ 1, 0.1 mM B'- γ 1 were titrated against 9 μM unmethylated PP2A core enzyme using VP-ITC microcalorimeter (MicroCal). All proteins were prepared in a buffer containing 25 mM HEPES, pH 8.0, and 150 mM NaCl. The data were fitted by software Origin 7.0.

Supplemental Data

Supplemental data include two figures and can be found with this article online at <http://www.cell.com/cgi/content/full/127/6/1239/DC1/>.

ACKNOWLEDGMENTS

We thank A. Saxena at BNL NSLS beamlines for help. This work was supported by grants from the US National Institutes of Health (Y.S.).

Received: October 19, 2006

Revised: November 20, 2006

Accepted: November 28, 2006

Published: December 14, 2006

REFERENCES

- Arino, J., Woon, C.W., Brautigam, D.L., Miller, T.B., Jr., and Johnson, G.L. (1988). Human liver phosphatase 2A: cDNA and amino acid sequence of two catalytic subunit isotypes. *Proc. Natl. Acad. Sci. USA* 85, 4252–4256.
- Bayliss, R., Littlewood, T., and Stewart, M. (2000). Structural basis for the interaction between FxFG nucleoporin repeats and importin-beta in nuclear trafficking. *Cell* 102, 99–108.
- Brunger, A.T., Adams, P.D., Clore, G.M., Delano, W.L., Gros, P., Grosse-Kunstleve, R.W., Jiang, J.S., Kuszewski, J., Nilges, M., Pannu, N.S., et al. (1998). Crystallography and NMR system: A new software suite for macromolecular structure determination. *Acta Crystallogr. D. Biol. Crystallogr.* 54, 905–921.
- Bryant, J.C., Westphal, R.S., and Wadzinski, B.E. (1999). Methylated C-terminal leucine residue of PP2A catalytic subunit is important for binding of regulatory B α subunit. *Biochem. J.* 339, 241–246.
- Calin, G.A., di Iasio, M.G., Caprini, E., Vorechovsky, I., Natali, P.G., Sozzi, G., Croce, C.M., Barbanti-Brodano, G., Russo, G., and Negrini, M. (2000). Low frequency of alterations of the alpha (PPP2R1A) and beta (PPP2R1B) isoforms of the subunit A of the serine-threonine phosphatase 2A in human neoplasms. *Oncogene* 19, 1191–1195.

- Chen, W., Possemato, R., Campbell, K.T., Plattner, C.A., Pallas, D.C., and Hahn, W.C. (2004). Identification of specific PP2A complexes involved in human cell transformation. *Cancer Cell* 5, 127–136.
- Cho, U.S., and Xu, W. (2006). Crystal structure of a protein phosphatase 2A heterotrimeric holoenzyme. *Nature*, *Epub ahead of print*.
- Colella, S., Ohgaki, H., Ruediger, R., Yang, F., Nakamura, M., Fujisawa, H., Kleihues, P., and Walter, G. (2001). Reduced expression of the A α subunit of protein phosphatase 2A in human gliomas in the absence of mutations in the A α and A β subunit genes. *Int. J. Cancer* 93, 798–804.
- Conti, E., Uy, M., Leighton, L., Blobel, G., and Kuriyan, J. (1998). Crystallographic analysis of the recognition of a nuclear localization signal by the nuclear import factor karyopherin α . *Cell* 94, 193–204.
- Graham, T.A., Weaver, C., Mao, F., Kimelman, D., and Xu, W. (2000). Crystal structure of a beta-catenin/Tcf complex. *Cell* 103, 885–896.
- Green, D.D., Yang, S.I., and Mumby, M.C. (1987). Molecular cloning and sequence analysis of the catalytic subunit of bovine type 2A protein phosphatase. *Proc. Natl. Acad. Sci. USA* 84, 4880–4884.
- Groves, M.R., Hanlon, N., Turowski, P., Hemmings, B.A., and Barford, D. (1999). The structure of the protein phosphatase 2A PR65/A subunit reveals the conformation of its 15 tandemly repeated HEAT motifs. *Cell* 96, 99–110.
- Hemmings, B.A., Adams-Pearson, C., Maurer, F., Muller, P., Goris, J., Merlevede, W., Hofsteenge, J., and Stone, S.R. (1990). α - and β -forms of the 65-kDa subunit of protein phosphatase 2A have a similar 39 amino acid repeating structure. *Biochemistry* 29, 3166–3173.
- Holm, L., and Sander, C. (1993). Protein structure comparison by alignment of distance matrices. *J. Mol. Biol.* 233, 123–138.
- Huber, A.H., Nelson, W.J., and Weis, W.I. (1997). Three-dimensional structure of the armadillo repeat region of beta-catenin. *Cell* 90, 871–882.
- Hunter, T. (1995). Protein kinases and phosphatases: the yin and yang of protein phosphorylation and signaling. *Cell* 80, 225–236.
- Ito, A., Kataoka, T.R., Watanabe, M., Nishiyama, K., Mazaki, Y., Sabe, H., Kitamura, Y., and Nojima, H. (2000). A truncated isoform of the PP2A B56 subunit promotes cell motility through paxillin phosphorylation. *EMBO J.* 19, 562–571.
- Ito, A., Koma, Y., Watabe, K., Nagano, T., Endo, Y., Nojima, H., and Kitamura, Y. (2003). A truncated isoform of the protein phosphatase 2A B56gamma regulatory subunit may promote genetic instability and cause tumor progression. *Am. J. Pathol.* 162, 81–91.
- Janssens, V., and Goris, J. (2001). Protein phosphatase 2A: a highly regulated family of serine/threonine phosphatases implicated in cell growth and signalling. *Biochem. J.* 353, 417–439.
- Janssens, V., Jordens, J., Stevens, I., Van Hoof, C., Martens, E., De Smedt, H., Engelborghs, Y., Waelkens, E., and Goris, J. (2003). Identification and functional analysis of two Ca²⁺-binding EF-hand motifs in the B⁵⁶/PR72 subunit of protein phosphatase 2A. *J. Biol. Chem.* 278, 10697–10706.
- Janssens, V., Goris, J., and Van Hoof, C. (2005). PP2A: the expected tumor suppressor. *Curr. Opin. Genet. Dev.* 15, 34–41.
- Jones, T.A., Zou, J.-Y., Cowan, S.W., and Kjeldgaard, M. (1991). Improved methods for building protein models in electron density maps and the location of errors in these models. *Acta Crystallogr. A* 47, 110–119.
- Kamibayashi, C., Lickteig, R.L., Estes, R., Walter, G., and Mumby, M.C. (1992). Expression of the A subunit of protein phosphatase 2A and characterization of its interactions with the catalytic and regulatory subunits. *J. Biol. Chem.* 267, 21864–21872.
- Kamibayashi, C., Estes, R., Lickteig, R.L., Yang, S.I., Craft, C., and Mumby, M.C. (1994). Comparison of heterotrimeric protein phosphatase 2A containing different B subunits. *J. Biol. Chem.* 269, 20139–20148.
- Kitajima, T.S., Sakuno, T., Ishiguro, K., Iemura, S., Natsume, T., Kawashima, S.A., and Watanabe, Y. (2006). Shugoshin collaborates with protein phosphatase 2A to protect cohesin. *Nature* 441, 46–52.
- Kloeker, S., Bryant, J.C., Strack, S., Colbran, R.J., and Wadzinski, B.E. (1997). Carboxymethylation of nuclear protein serine/threonine phosphatase X. *Biochem. J.* 327, 481–486.
- Koma, Y.I., Ito, A., Watabe, K., Kimura, S.H., and Kitamura, Y. (2004). A truncated isoform of the PP2A B56gamma regulatory subunit reduces irradiation-induced Mdm2 phosphorylation and could contribute to metastatic melanoma cell radioresistance. *Histol. Histopathol.* 19, 391–400.
- Kraulis, P.J. (1991). Molscript: a program to produce both detailed and schematic plots of protein structures. *J. Appl. Crystallogr.* 24, 946–950.
- Lechward, K., Awotunde, O.S., Swiatek, W., and Muszynska, G. (2001). Protein phosphatase 2A: variety of forms and diversity of functions. *Acta Biochim. Pol.* 48, 921–933.
- Li, X., and Virshup, D.M. (2002). Two conserved domains in regulatory B subunits mediate binding to the A subunit of protein phosphatase 2A. *Eur. J. Biochem.* 269, 546–552.
- McCoy, A.J., Grosse-Kunstleve, R.W., Storoni, L.C., and Read, R.J. (2005). Likelihood-enhanced fast translation functions. *Acta Crystallogr. D* 61, 458–464.
- Nicholls, A., Sharp, K.A., and Honig, B. (1991). Protein folding and association: insights from the interfacial and thermodynamic properties of hydrocarbons. *Proteins* 11, 281–296.
- Otwinowski, Z., and Minor, W. (1997). Processing of X-ray diffraction data collected in oscillation mode. *Methods Enzymol.* 276, 307–326.
- Riedel, C.G., Katis, V.L., Katou, Y., Mori, S., Itoh, T., Helmhart, W., Galova, M., Petronczki, M., Gregan, J., Cetin, B., et al. (2006). Protein phosphatase 2A protects centromeric sister chromatid cohesion during meiosis I. *Nature* 441, 53–61.
- Ruediger, R., Roeckel, D., Fait, J., Bergqvist, A., Magnusson, G., and Walter, G. (1992). Identification of binding sites on the regulatory A subunit of protein phosphatase 2A for the catalytic C subunit and for tumor antigens of simian virus 40 and polyomavirus. *Mol. Cell. Biol.* 12, 4872–4882.
- Ruediger, R., Hentz, M., Fait, J., Mumby, M., and Walter, G. (1994). Molecular model of the A subunit of protein phosphatase 2A: interaction with other subunits and tumor antigens. *J. Virol.* 68, 123–129.
- Ruediger, R., Pham, H.T., and Walter, G. (2001a). Alterations in protein phosphatase 2A subunit interaction in human carcinomas of the lung and colon with mutations in the A beta subunit gene. *Oncogene* 20, 1892–1899.
- Ruediger, R., Pham, H.T., and Walter, G. (2001b). Disruption of protein phosphatase 2A subunit interaction in human cancers with mutations in the A alpha subunit gene. *Oncogene* 20, 10–15.
- Stone, S.R., Hofsteenge, J., and Hemmings, B.A. (1987). Molecular cloning of cDNAs encoding two isoforms of the catalytic subunit of protein phosphatase 2A. *Biochemistry* 26, 7215–7220.
- Suzuki, K., and Takahashi, K. (2003). Reduced expression of the regulatory A subunit of serine/threonine protein phosphatase 2A in human breast cancer MCF-7 cells. *Int. J. Oncol.* 23, 1263–1268.
- Takagi, Y., Futamura, M., Yamaguchi, K., Aoki, S., Takahashi, T., and Saji, S. (2000). Alterations of the PPP2R1B gene located at 11q23 in human colorectal cancers. *Gut* 47, 268–271.
- Tang, Z., Shu, H., Qi, W., Mahmood, N.A., Mumby, M.C., and Yu, H. (2006). PP2A is required for centromeric localization of Sgo1 and proper chromosome segregation. *Dev. Cell* 10, 575–585.

Tolstykh, T., Lee, J., Vafai, S., and Stock, J.B. (2000). Carboxyl methylation regulates phosphoprotein phosphatase 2A by controlling the association of regulatory B subunits. *EMBO J.* 19, 5682–5691.

Virshup, D.M. (2000). Protein phosphatase 2A: a panoply of enzymes. *Curr. Opin. Cell Biol.* 12, 180–185.

Walter, G., Ferre, F., Espiritu, O., and Carbone-Wiley, A. (1989). Molecular cloning and sequence of cDNA encoding polyoma medium tumor antigen-associated 61-kDa protein. *Proc. Natl. Acad. Sci. USA* 86, 8669–8672.

Wang, S.S., Esplin, E.D., Li, J.L., Huang, L., Gazdar, A., Minna, J., and Evans, G.A. (1998). Alterations of the PPP2R1B gene in human lung and colon cancer. *Science* 282, 284–287.

Wei, H., Ashby, D.G., Moreno, C.S., Ogris, E., Yeong, F.M., Corbett, A.H., and Pallas, D.C. (2001). Carboxymethylation of the PP2A catalytic subunit in *Saccharomyces cerevisiae* is required for efficient interaction with the B-type subunits Cdc55p and Rts1p. *J. Biol. Chem.* 276, 1570–1577.

Wu, J., Tolstykh, T., Lee, J., Boyd, K., Stock, J.B., and Broach, J.R. (2000). Carboxyl methylation of the phosphoprotein phosphatase 2A

catalytic subunit promotes its functional association with regulatory subunits in vivo. *EMBO J.* 19, 5672–5681.

Xing, Y., Xu, Y., Chen, Y., Jeffrey, P.D., Chao, Y., Zheng, L., Li, Z., Strack, S., Stock, J.B., and Shi, Y. (2006). Structure of Protein Phosphatase 2A Core Enzyme Bound to Tumor-inducing Toxins. *Cell* 127, 341–352.

Yu, X.X., Du, X., Moreno, C.S., Green, R.E., Ogris, E., Feng, Q., Chou, L., McQuoid, M.J., and Pallas, D.C. (2001). Methylation of the protein phosphatase 2A catalytic subunit is essential for association of Balph regulatory subunit but not SG2NA, striatin, or polyomavirus middle tumor antigen. *Mol. Biol. Cell* 12, 185–199.

Accession Numbers

The atomic coordinates of the three PP2A holoenzyme complexes have been deposited in the Protein Data Bank with the accession codes 2NPP (full-length C α), 2NYM (truncated C α and B'- γ 3), and 2NYL (truncated C α and B'- γ 1).